

# 317. Analysis of Insertion Process for Robotic Assembly

S. Kilikevičius<sup>1,a</sup>, B. Bakšys<sup>2,b</sup>

<sup>1,2</sup> Kaunas University of Technology, Department of Mechatronics, Kęstučio st. 27, LT-44025 Kaunas, Lithuania.

E-mail: <sup>a</sup> sigitas.kilikevicius@stud.ktu.lt, <sup>b</sup> bronius.baksys@ktu.lt

(Received 16 August 2007; accepted 10 October 2007)

**Abstract.** Insertion process of cylindrical parts with clearance for robotic assembly using vibratory excitation is analyzed in the paper. Mathematical model of vibratory parts insertion process, which determines peg contact with the chamfer of the bush, peg one point and two point contact with the bush hole, was formed. Simulation of cylindrical parts insertion process was performed. The influence of vibrations on the insertion process, when mobile based peg is kinematically excited in axial direction, was determined. The combinations of excitation and system parameters, under which insertion process duration is the shortest and the process is the most reliable, were detected.

**Keywords:** peg-in-hole, vibrations, robotic assembly, simulation.

## 1. Introduction

Successful and competitive manufacture requires to increase productivity, reduce equipment cost and ensure maximal quality. The variety of productivity requires more flexibility in assembly systems, so implementation of industrial robots into automated assembly systems is unavoidable. The effective solution for increasing the productivity of assembly operations is to increase the insertion speed. It is possible to achieve high insertion speed using modern robotic technology for assembly operations. However, the problems such as wedging and jamming occur, under high insertion speed, which should be avoided. Quasi-static model of parts insertion, analyzed in the majority of papers [1, 2], is not suitable for research of high speed insertion process.

Paper [3] investigates high speed insertion process, diagrams of variation in time of insertion forces, tilt angle of peg, lateral deviation along the horizontal direction and depth of insertion are given. It was noticed that the motion of mobile based peg during two point contact stage is uneven. The influence of different parameters on tilt angle of the peg and insertion forces was determined, but diagrams of their dependences were not given. Mathematical model of insertion was presented in paper [4]. Conditions for the shortest duration and the highest reliability of insertion process were determined.

High insertion speed causes high insertion forces, therefore the probability of jamming increases. When the parts to be assembled get jammed, assembly equipment damages, manufacture disconcerts. Jamming can be

avoided by exiting vibrations of the parts to be assembled [5].

A device for high speed and precision chamferless assembly, using vibratory technology, is proposed in paper [6]. The device consists of work table, driven by vibratory motion, provided by two pneumatic bellows actuators, piloted by the pseudo-random binary signal, and dynamic compliance device. However, design of the proposed device is quite complex. The influence of insertion parameters on insertion process was not determined in the paper. Also the influence of vibration on insertion process and its duration was not determined.

In order the process of vibratory assembly to be reliable and effective, it is necessary to ensure that the parameters, which make an influence on insertion process, were rationally selected.

This paper investigates the insertion of mobile based peg into immobile based bush with guaranteed clearance, under kinematical excitation of the peg in axial direction. With properly selected parameters of kinematical excitation it is possible to avoid insertion process failures due to jamming and to obtain minimal duration of the insertion process.

## 2. Mathematical model of parts insertion process

Insertion of mobile based peg, which is moved in constant velocity  $v$  by robot, into immobile bush is investigated (Fig. 1). Robot arm is equipped with remote centre compliance (RCC) device and gripper. The peg is hold by the gripper and only can turn around the centre of compli-

ance  $C$  and slip in radial direction. The gripper is excited by vibration of amplitude  $A_e$  and frequency  $\omega$ , in  $z$  axis direction. These vibrations are transferred to the peg through elastic elements. This kind of excitation is called kinematical.

Vibratory excitation force  $F_e$ , elastic component of the insertion force along  $x$  axis  $F_x$ , along  $z$  axis  $F_z$  and torsion moment  $M$  about point  $C$  act in the centre of compliance.

Insertion process can be divided into three stages: chamfer crossing stage, one point contact and two point contact stages.

During the assembly process, the peg axis and the hole misalign by distance  $\varepsilon$  due to positional errors, therefore sliding downward the peg touches the chamfer. Then insertion process starts (Fig. 2, a). During the chamfer crossing stage (Fig. 2, b), the peg is influenced by elastic components of insertion force and torque ( $F_x, F_z, M$ ), vibratory excitation force  $F_e \sin \omega t$ , gravity  $mg$ , inertia forces  $m\ddot{x}_G, m\ddot{z}_G$ , inertia torque  $I\ddot{\theta}$ , reaction force  $F_n$ , friction force  $\mu F_n$ ; where  $m$  is the mass of the peg and the gripper,  $I$  is inertia moment of the peg and the gripper about mass centre,  $g$  is gravitational constant,  $\mu$  is dry friction constant,  $x_G, z_G$  are the coordinates of the mass centre.

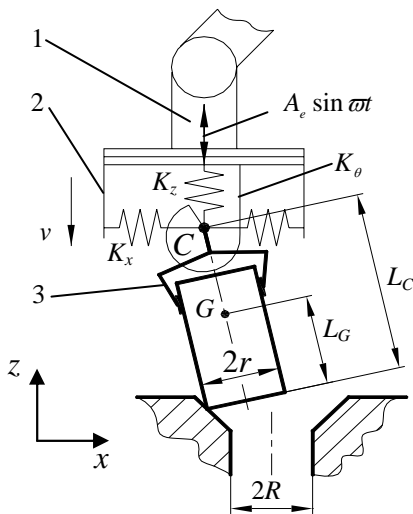


Fig. 1. Scheme of vibratory insertion: 1 – robot arm; 2 – RCC device; 3 – gripper

Applying D'Alembert principle, movement of the peg during the chamfer crossing stage is determined by the following equations:

$$\left. \begin{aligned} K_1 F_n - F_x - m\ddot{x}_G &= 0 \\ K_2 F_n - F_z - F_e \sin \omega t - m\ddot{z}_G - mg &= 0 \\ (F_x \cos \theta + F_z \sin \theta + F_e \sin \omega t \sin \theta)(L_C - L_G) + \\ + K_3 F_n - M - I\ddot{\theta} &= 0 \end{aligned} \right\} \quad (1)$$

where  $K_1 = \sin \alpha - \mu \cos \alpha$ ;  $K_2 = \cos \alpha + \mu \sin \alpha$ ;

$K_3 = (L_G K_1 - r K_2) \cos \theta + (L_G K_2 + r K_1) \sin \theta$ ;  $\alpha$  is the chamfer angle;  $L_G$  is the distance from the lower end surface of the peg to the centre of mass;  $L_C$  is the distance to the center of compliance;  $\theta$  is tilt angle of the peg;  $\theta_0$  is tilt angle of the peg at the initial instant of time;  $K_x, K_z, K_\theta$  are lateral stiffness, axial stiffness and angular stiffness respectively.

The peg slides down the chamfer until cylindrical surface of the peg touches the hole. Insertion process steps into the one point contact stage (Fig. 3, a). After the evaluation of acting forces in the one point contact stage (Fig. 3, b), movement of the peg in the hole is determined by the following equations:

$$\left. \begin{aligned} K_4 F_n - F_x - m\ddot{x}_G &= 0 \\ K_5 F_n - F_z - F_e \sin \omega t - m\ddot{z}_G - mg &= 0 \\ (F_x \cos \theta + F_z \sin \theta + F_e \sin \omega t \sin \theta)(L_C - L_G) + \\ + (L_G - h - \mu r) F_n - M - I\ddot{\theta} &= 0 \end{aligned} \right\} \quad (2)$$

where  $K_4 = \cos \theta - \mu \sin \theta$ ;  $K_5 = \sin \theta + \mu \cos \theta$ ;  $h$  is insertion depth.

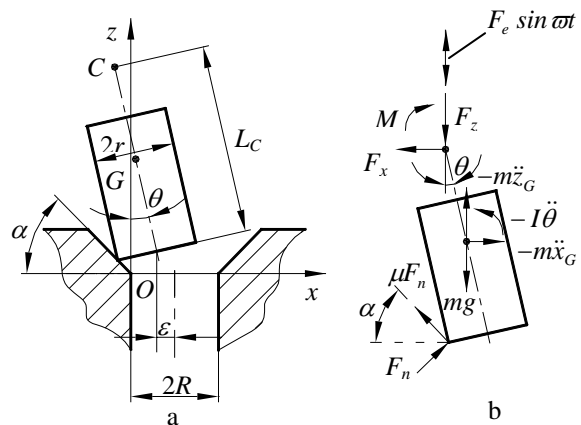


Fig. 2. Peg and chamfer contact

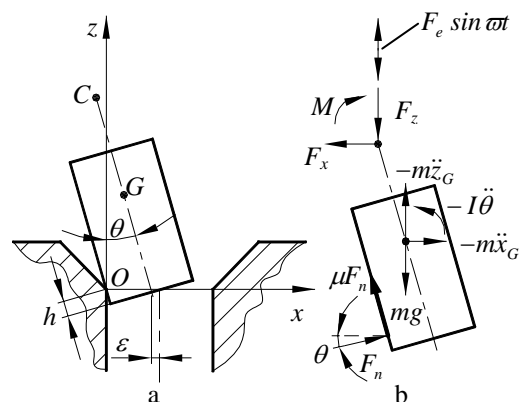


Fig. 3. One point contact stage

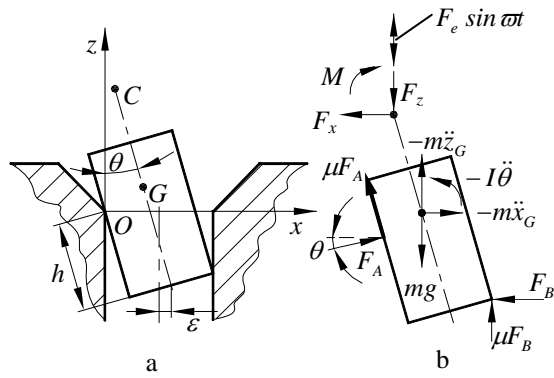


Fig. 4. Two point contact stage

The peg contacts with the hole in one point until the lower edge of the peg reaches internal surface of the hole. Insertion process steps into the two point contact stage (Fig. 4, a). After the evaluation of acting forces in the one point contact stage (Fig. 4, b), movement of the peg in the hole is determined by the following equations:

$$\left. \begin{aligned} K_4 F_A - F_B - F_x - m\ddot{x}_G &= 0 \\ K_5 F_A + \mu F_B - F_z - F_e \sin \omega t - m\ddot{z}_G - mg &= 0 \\ (F_x \cos \theta + F_z \sin \theta + F_e \sin \omega t \sin \theta)(L_C - L_G) - M - \\ - I\ddot{\theta} + (L_G - h - \mu r)F_A - (L_G K_4 - r K_5)F_B &= 0 \end{aligned} \right\} (3)$$

The parts are completely assembled when the required depth of insertion  $h_i$  is reached.

### 3. Simulation of insertion process

Programs for the simulation of insertion process were written using MatLab software. The following initial values of the parameters of insertion process were used:  $m = 0.1$  kg,  $r = 0.0099$  m,  $R = 0.01$  m,  $I = 0.002$  kg·m<sup>2</sup>,  $L_G = 0.05$  m,  $L_C = 0.025$  m,  $\alpha = \pi/4$  rad,  $\mu = 0.1$ ,  $v = 0.1$  m/s,  $\theta_0 = 0.01$  rad,  $\dot{\theta}_0 = 0.01$  rad/s,  $\varepsilon_0 = -0.001$  m,  $\dot{\varepsilon}_0 = 0.001$  m/s,  $K_x = 2000$  N/m,  $K_z = 10000$  N/m,  $K_\theta = 20$  Nm/rad,  $h_i = 0.05$  m.

Total insertion duration  $t_3$  is the duration from the beginning of insertion process until the parts are completely inserted. It consists of the chamfer crossing duration, one point contact duration and two point contact duration. The most effective way to shorten insertion process duration  $t_3$ , and to increase the productivity of assembly operations, is to increase the insertion speed. When insertion speed is increasing, the insertion process duration distinctly shortens (Fig. 5, a). Jumps of insertion process duration  $t_3$ , visible in diagram, occur due to uneven movement of the peg in the hole. Dependences of insertion process duration on insertion speed, under kinematical excitation of mobile based part by vibration amplitude  $A_e = 0.5 \cdot 10^{-3}$  m and frequency  $\omega = 100$  s<sup>-1</sup>, were determined (Fig. 5, b). The results showed that the insertion process duration is shorter under kinematical excitation of mobile based part and properly selected excitation parameters.

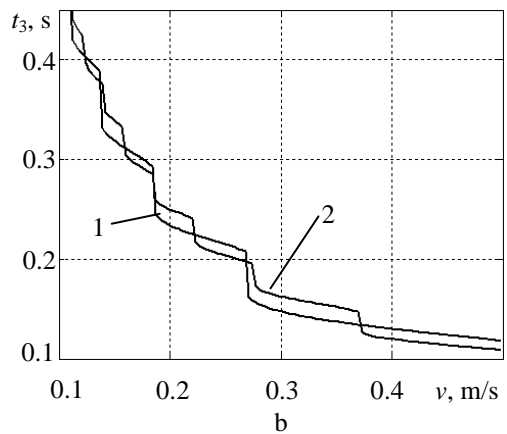
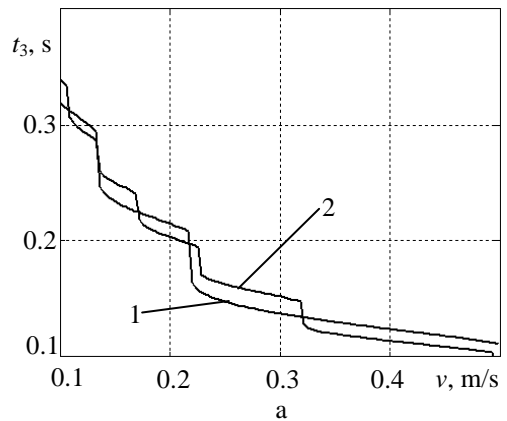


Fig. 5. Dependences of insertion process duration  $t_3$  on insertion speed  $v$ : a – under kinematical excitation of mobile based part; b – without using vibrations, under different values of axial stiffness: 1 –  $K_z = 2 \cdot 10^3$  N/m; 2 –  $K_z = 5 \cdot 10^3$  N/m

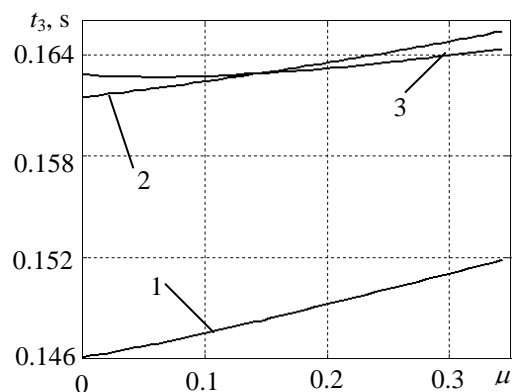
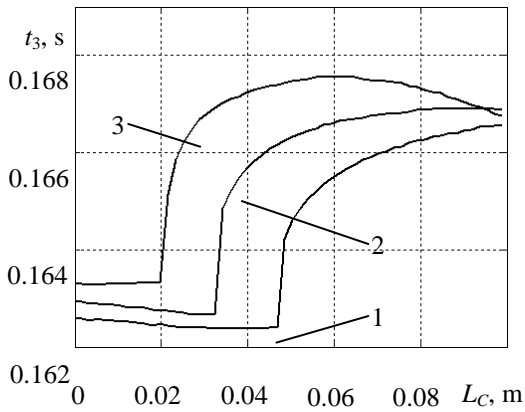


Fig. 6. Dependences of insertion process duration  $t_3$  on coefficient of friction  $\mu$ , under different axial stiffness: 1 –  $K_z = 0.5 \cdot 10^3$  N/m; 2 –  $K_z = 2 \cdot 10^3$  N/m; 3 –  $K_z = 5 \cdot 10^3$  N/m



**Fig. 7.** Dependences of insertion process duration  $t_3$  on  $L_C$ , under different lateral stiffness: 1 –  $K_x = 2 \cdot 10^3$  N/m; 2 –  $K_x = 3 \cdot 10^3$  N/m; 3 –  $K_x = 5 \cdot 10^3$  N/m

The insertion process takes more time when the coefficient of friction is increasing (Fig. 6). Duration of the insertion process is the most reasonable when the distance from the lower end surface of the peg to the centre of compliance  $L_C$  is close to 0 (Fig. 7). The parameters of excitation have a noticeable influence on insertion duration, under assembly process with kinematical excitation. When excitation frequency is increasing, the insertion process duration unevenly decreases (Fig. 8, a). Excitation amplitude has more noticeable influence on the insertion process duration. The duration of insertion process  $t_3$  increases when excitation amplitude  $A_e$  is increasing (Fig. 8, b). It increases because the amplitude of uneven movement of the peg increases under the influence of higher excitation amplitude.

Insertion process can fail due to jamming. Connection of jammed parts is possible by removing the causes of jamming. For this purpose, axial vibration of the peg can be excited. Due to this, balance of acting forces and moments on the peg changes and insertion process continues. The effect of vibratory excitation is clearly represented by hatched areas of distance  $L_C$  and axial stiffness  $K_z$  combinations, under which the peg is not completely inserted into the bush hole (Fig. 9). Without using vibrations (Fig 9, area 1), the peg gets jammed under high values of distance  $L_C$ , therefore insertion process is not finished. When mobile based part is kinematically excited in axial direction by vibration amplitude  $A_e = 0.5 \cdot 10^{-3}$  m and frequency  $\omega = 100$  s<sup>-1</sup>, the area of not successful insertion distinctly decreases (Fig. 9, area 2). The parts are not completely connected only in the narrow area, under very high values of distance  $L_C$  and low values of axial stiffness  $K_z$ .

In order the insertion process of vibratory assembly to run reliably, it is necessary to select properly the values of vibration amplitude and frequency. Areas which represent the combinations of excitation amplitude  $A_e$  and frequency  $\omega$ , under which the parts get jammed, are shown in Fig. 10. Following from an arrangement of the areas, it is advantageous to select lower values of excitation amplitude. The parts do not connect under low excitation frequency, besides under excitation frequency  $\omega = 35\text{--}50$  s<sup>-1</sup> and high

excitation amplitude, the area of not stable insertion emerges. Consequently, higher vibratory excitation frequency ensures more favorable conditions for the insertion process.

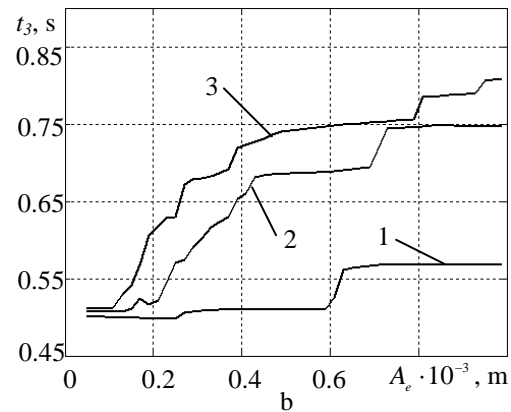
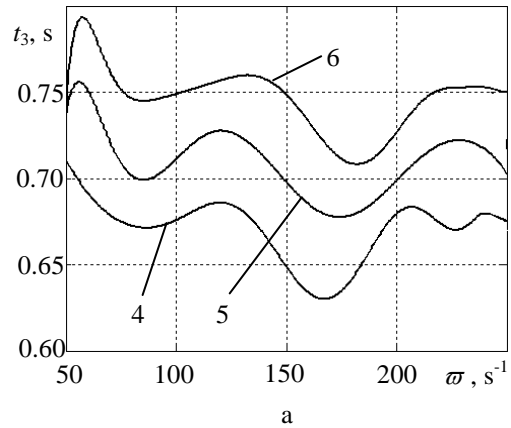


**Fig. 8.** Dependences of insertion process duration  $t_3$ : a – on excitation frequency; b – on excitation amplitude, under different axial stiffness: 1 –  $K_z = 2 \cdot 10^3$  N/m; 2 –  $K_z = 5 \cdot 10^3$  N/m; 3 –  $K_z = 8 \cdot 10^3$  N/m; 4 –  $K_z = 2 \cdot 10^4$  N/m; 5 –  $K_z = 2.5 \cdot 10^4$  N/m; 6 –  $K_z = 3 \cdot 10^4$  N/m

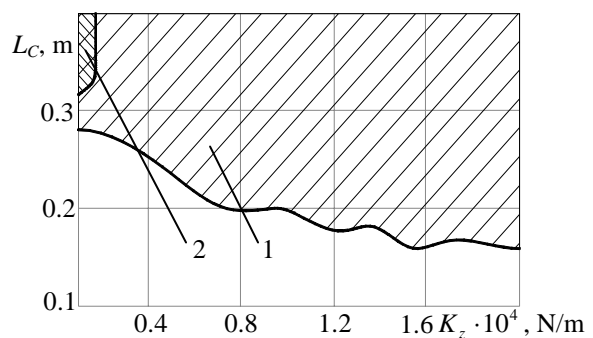


**Fig. 9.** Areas of distance  $L_C$  and axial stiffness  $K_z$  combinations when the parts are not connected (hatched): 1 – without using vibrations; 2 – under kinematical excitation of mobile based part

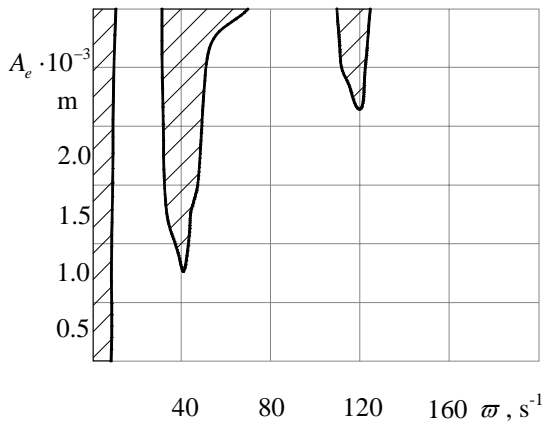


**Fig. 10.** Areas of excitation amplitude  $A_e$  and frequency  $\omega$  combinations when jammed parts are not connected (hatched),  $K_z = 2.5 \cdot 10^3$  N/m,  $L_C = 0.4$  m

Distance  $L_C$  to the centre of compliance makes high influence on jamming. Under kinematical excitation, mobile based part can not be inserted into the base part only when excitation frequency is too low (Fig. 11, a), the value of excitation amplitude and distance  $L_C$  (Fig. 11, b) is too high.

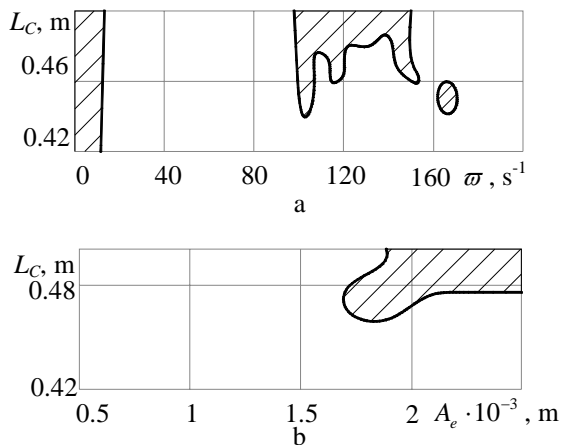


**Fig. 11.** Area, wherein parts get jammed (hatched), depending on distance to the centre of compliance  $L_C$  and a – excitation frequency  $\omega$ ; b – excitation amplitude  $A_e$ ;  $K_z = 3 \cdot 10^3$  N/m

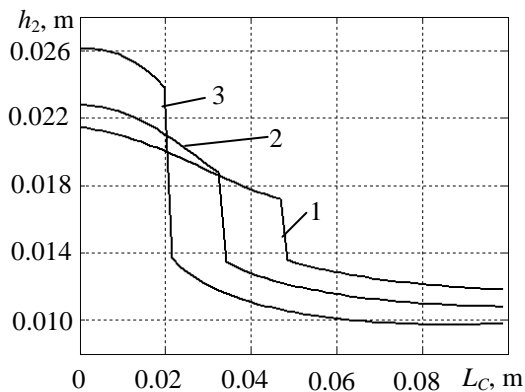


**Fig. 12.** Dependences of depth  $h_2$  on  $L_C$ , under different values of  $K_x$ : 1 –  $K_x = 2 \cdot 10^3$  N/m; 2 –  $K_x = 3 \cdot 10^3$  N/m; 3 –  $K_x = 5 \cdot 10^3$  N/m

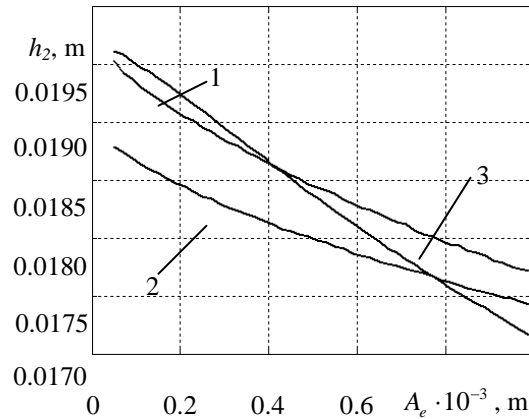


**Fig. 13.** Dependences of depth  $h_2$  on excitation amplitude, under different axial stiffness: 1 –  $K_z = 2 \cdot 10^3$  N/m; 2 –  $K_z = 5 \cdot 10^3$  N/m; 3 –  $K_z = 8 \cdot 10^3$  N/m

It is noticed, that wedging usually appears when the two point contact appears in a small depth. Besides, the probability increases that the peg will jump out of the hole when the two point contact appears in a small depth. Therefore, it is necessary to select such values of insertion process parameters, which influence the higher value of depth  $h_2$ . Depth  $h_2$  decreases when distance  $L_C$  is increasing (Fig. 12). When excitation amplitude is decreasing, the two point contact appears in higher depth (Fig. 13).

#### 4. Conclusions

The research showed that excitation of inserting peg vibrations has a positive effect on robotic assembly process. It is possible to shorten insertion process duration by changing the parameters of assembly system and excitation. Insertion process duration  $t_3$  decreases when excitation frequency  $\omega$  is increasing, excitation amplitude  $A_e$  and friction between the parts are decreasing, and distance  $L_C$  is close to 0. It is noticed that by using kinematical excitation in assembly process with properly selected excitation parameters, it is possible to decrease the probability of jamming and to increase the reliability of assembly. The simulation showed that jammed components are not connected when the values of excitation amplitude  $A_e$  and frequency  $\omega$  are too low. It was determined that the probability of wedging, jamming and peg jump out from the hole decreases, when distance  $L_C$  is decreasing and excitation amplitude is not very high.

## References

- [1] **Asada H., Kakumoto Y.** The Dynamic RCC Hand for High Speed Assembly. - Proc. of the 1988 IEEE Int. Conf. on Robotics and Automation. - Philadelphia, 1988, p. 120-125.
- [2] **Setchi R., Bratanov D.** Three-dimensional simulation of accommodation. - Assembly automation. Vol. 18. No. 4. - MCB University Press, 1998. p. 291-301.
- [3] **Du K. L., Zhang B. B., Huang X., Hu J.** Dynamic Analysis of Assembly Process with Passive Compliance for Robot Manipulators. - Proc. 2003 IEEE Int. Symposium on Computational Intelligence in Robotics and Automation. - Kobe, 2003. p. 1168-1173.
- [4] **Bakšys B., Kilikevičius S.** Insertion investigation of cylindrical parts to be assembled with clearance. - Mechanika. - Kaunas: Technologija, 2006, No. 2(58). p. 30-39.
- [5] **Bakšys B., Fedaravičius A., Povilionis A. B.** Connection Conditions of Mobile Based Parts. - Mechanika. - Kaunas: Technologija, 2002, No. 5(37). p. 19-25.
- [6] **Trong D. N., Betemps M., Jutard A.** Analysis of Dynamic Assembly Using Passive Compliance. - Proc. of the 1995 IEEE Int. Conf. on Robotics and Automation. - Nayoga, 1995, p. 1997-2002.